

# Dissipative quantum dynamics of fermions in optical lattices: a slave-spin approach

Jean-Sébastien Bernier,<sup>1,2</sup> Dario Poletti,<sup>3</sup> and Corinna Kollath<sup>4</sup>

<sup>1</sup>*Department of Physics and Astronomy, University of British Columbia, Vancouver V6T 1Z1, Canada.*

<sup>2</sup>*Pulse Energy, 600-576 Seymour Street, Vancouver V6B 3K1, Canada.*

<sup>3</sup>*Singapore University of Technology and Design, 20 Dover Drive, 138682 Singapore.*

<sup>4</sup>*University of Bonn, HISKP, Nussallee 14-16, 53115 Bonn, Germany*

We investigate the influence of a Markovian environment on the dynamics of interacting spinful fermionic atoms in a lattice. In order to explore the physical phenomena occurring at short times, we develop a method based on a slave-spin representation of fermions which is amenable to the investigation of the dynamics of dissipative systems. We apply this approach to two different dissipative couplings which can occur in current experiments: a coupling via the local density and a coupling via the local double occupancy. We complement our study based on this novel method with results obtained using the adiabatic elimination technique and with an exact study of a two-site model. We uncover that the decoherence is slowed down by increasing either the interaction strength or the dissipative coupling (the Zeno effect). We also find, for the coupling to the local double occupancy, that the final steady state can sustain single-particle coherence.

PACS numbers: 03.65.Yz, 03.75.Ss, 05.30.Fk

## I. INTRODUCTION

The behavior of physical systems is typically influenced by the surrounding environment. However, identifying the correct environmental mechanisms and their corresponding effects is quite often a difficult task. For example, the relevant environment can be as simple as external noises, like magnetic field fluctuations, but can also be system specific couplings such as electrons coupled to phononic modes in solids or cold atomic gases subjected to fluorescence scattering in near resonant optical lattices [1]. In fact, a large corpus of theoretical frameworks has been developed to describe the interactions between a system and its environment in various limits. This vast inventory ranges from the description of electron-phonon couplings using baths of harmonic oscillators, to the Markovian description of memory-less environments, a prevalent approach in the field of quantum optics. In recent years, the renewed interest for the physics of environmentally coupled systems has been fueled by the realization that environments can perturb non-trivially the central system by inducing, for example, superconductivity in solid state systems [2] or Zeno- and anti-Zeno effects in quantum optical systems [3]. Furthermore, state preparation by environmental coupling, which optical pumping is one of the most common implementations, has recently been generalized and promises to be a great avenue to realize intriguing states of matter [4–10]. The interest for these systems is compounded by the prediction of surprising effects such as the impeding of decoherence by dissipative coupling in bosonic gases under dephasing or atom losses [9, 11–15], the enhancement or appearance of distinct transport properties under the influence of globally acting dissipation (see e.g. [16, 17] and references therein), the presence of scaling regimes in the dissipative quantum dynamics [12, 15, 18–20], and the occurrence of glass-like dynamics in dissipatively coupled many-body systems [18, 21, 22]. Despite these impressive advances,

the interplay between the environmental coupling and the interacting many-body dynamics, and by extension the induced effects, are still not fully understood.

The development of a better comprehension for these systems, in particular for fermionic ones, has historically been hindered by a lack of proper theoretical methods to explore their rich physical structure. We develop here a novel method, based on a slave-spin representation of fermions [23], to uncover the physics of many-body systems coupled to Markovian environments. This newly developed approach proves to be extremely useful to investigate the short-time dynamics of a broad class of strongly interacting fermionic systems. We show its applicability to two different kinds of dissipative processes: environmental effects described by couplings to either the system density or double-occupancy. The coupling to the density of fermions is one of possible dissipative effects that can occur in ultracold fermionic gases in red-detuned optical lattices [11, 24] by fluorescence scattering. In order to engineer the coupling to the double occupancy, an interaction energy shift can be added [10], such that only doubly occupied sites are sensitive to a certain driven transition. Thus, our findings have wide implications for the stability of complex quantum states in realizable experiments. We also supplement the developed approach with comparisons to exact diagonalization and adiabatic elimination methods [25–27] applied to the same dissipative many-body systems.

The rest of the article is structured as follows: in section II, we present the model and the considered dissipative couplings with their corresponding asymptotic long-time steady states. In section III, we introduce the different theoretical approaches. We describe in III A the exact diagonalization approach, in III B the newly developed slave-particle approach, and in III C the adiabatic elimination method. In section IV, we present our results for the coupling to the two different environments: in IV A, the coupling to a local dephasing noise is inves-

tigated, whereas in IV B we consider the local coupling to doubly occupied sites. The various arising effects, the Zeno effect, the slowing down of decoherence and its oscillating behavior in the presence of strong interaction, are discussed within this section. Finally, we conclude in section V.

## II. DESCRIPTION OF THE SYSTEM AND ITS STEADY STATE

### A. Model

We investigate the Hamiltonian evolution of interacting fermions in a lattice potential described by the  $d$ -dimensional Hubbard model

$$H = -J \sum_{\mathbf{r}, \mathbf{r}'(\mathbf{r}), \sigma} \left( c_{\mathbf{r}, \sigma}^\dagger c_{\mathbf{r}', \sigma} + \text{h.c.} \right) + \frac{U}{2} \sum_{\mathbf{r}} (n_{\mathbf{r}, \uparrow} + n_{\mathbf{r}, \downarrow} - 1)^2 \quad (1)$$

where  $c_{\mathbf{r}, \sigma}^\dagger$  is the creation operator for a fermion with spin  $\sigma = \{\uparrow, \downarrow\}$  and site index  $\mathbf{r}$ ,  $n_{\mathbf{r}, \sigma} = c_{\mathbf{r}, \sigma}^\dagger c_{\mathbf{r}, \sigma}$  is the density operator. Here  $\mathbf{r}'(\mathbf{r})$  denotes all nearest-neighbors of site  $\mathbf{r}$ . The first term in Eq. (1) corresponds to the kinetic energy of the fermions and  $J > 0$  is the hopping coefficient. The second term characterizes the repulsive interaction with strength  $U > 0$ . This model is often used to describe fermionic atoms confined to optical lattice potentials [28, 29] or electrons in solids [30].

In addition to the unitary dynamics, we consider the presence of different couplings to the environment causing a dissipative evolution. For Markovian processes, the evolution of the density matrix,  $\rho$ , describing the fermions follows a master equation

$$\frac{d}{dt} \rho(t) = -\frac{i}{\hbar} [H, \rho(t)] + \mathcal{D}(\rho(t)). \quad (2)$$

The first term on the right hand side of Eq.(2) corresponds to the unitary evolution induced by the Hamiltonian. The second term models the dissipative coupling. The effects of the considered environments are described by dissipators within the Lindblad formalism, i.e.

$$\mathcal{D}(\rho) = \gamma \sum_{\mathbf{r}, \sigma} \left( j_{\mathbf{r}, \sigma} \rho j_{\mathbf{r}, \sigma}^\dagger - \frac{1}{2} j_{\mathbf{r}, \sigma}^\dagger j_{\mathbf{r}, \sigma} \rho - \frac{1}{2} \rho j_{\mathbf{r}, \sigma}^\dagger j_{\mathbf{r}, \sigma} \right) \quad (3)$$

where  $j_{\mathbf{r}, \sigma}$  denotes the quantum jump operators.

We consider here two types of dissipative environment. These environments, chosen for the interesting dynamical effects they induce, are described within the Lindblad formalism using the following quantum jump operators:

- (i) the local density

$$j_{\mathbf{r}, \sigma} = n_{\mathbf{r}, \sigma}; \quad (4)$$

- (ii) the local double occupancy density

$$j_{\mathbf{r}, \sigma} = \frac{1}{\sqrt{2}} n_{\mathbf{r}, \uparrow} n_{\mathbf{r}, \downarrow}. \quad (5)$$

In the analysis that follows, we typically consider the situation where the system is initially prepared in the ground state of the Fermi-Hubbard model, and then the coupling to the environment is switched on. Our study focuses on the time evolution of the system which, as we will present in details, strongly depends on the interplay of the unitary and dissipative dynamics.

### B. Structure of the decoherence free subspaces and steady states

The two different dissipative couplings exemplify well two distinct situations:

- (i) the local density coupling has a unique steady state towards which *any* initial state evolves;
- (ii) the local double occupancy coupling has an entire subspace of steady states and the asymptotic long time state depends on the initial condition.

For case (i) the decoherence free subspace of the dissipator, defined by  $\mathcal{D}(\rho) = 0$ , is given by all density matrices which are diagonal within the Fock basis. For these density matrices the first term in the dissipator Eq. (3) is exactly canceled by the last two terms. This implies that without the Hamiltonian evolution, i.e.  $H = 0$ , the entire set of diagonal density matrices are steady states ( $\dot{\rho} = 0$ ). While the interaction part of the Hamiltonian leaves these states untouched, the competing kinetic term lifts this degeneracy. As a consequence, only the infinite temperature state, i.e. the state proportional to unity in the Fock basis, is invariant under the combined action of the dissipator and of the Hamiltonian. As we will later use the representation of this steady state as a reduced single site density matrix  $\tilde{\rho}$  (where one traces out all sites except one), we provide here its definition in the single site Fock basis

$$\tilde{\rho}(t) = \sum_{m=0, \uparrow, \downarrow, \uparrow\downarrow} \tilde{\rho}_m(t) |m\rangle \langle m| \quad (6)$$

$$\tilde{\rho}_0(t = \infty) = (1 - \bar{n}_\uparrow)(1 - \bar{n}_\downarrow) \quad (7)$$

$$\tilde{\rho}_\uparrow(t = \infty) = \bar{n}_\uparrow(1 - \bar{n}_\downarrow) \quad (8)$$

$$\tilde{\rho}_\downarrow(t = \infty) = (1 - \bar{n}_\uparrow)\bar{n}_\downarrow \quad (9)$$

$$\tilde{\rho}_{\uparrow\downarrow}(t = \infty) = \bar{n}_\uparrow\bar{n}_\downarrow. \quad (10)$$

where  $\bar{n}_\sigma$  denotes the average density for the fermions with spin  $\sigma$ . It is important to note that we are considering here an infinite homogeneous system in any dimension.

For case (ii), where the environment effectively couples to the local double occupancy, the situation is very different. Here the decoherence free subspace is much larger.

It contains the diagonal matrices in Fock space, but additionally, states which have no double occupancies, but still coherence. Since the interaction does not affect this subclass of states, all states belonging to this subspace and that are additionally eigenstates of the kinetic term of the Hamiltonian are steady states. The infinite temperature state is one of these steady states. However, the actual steady state reached depends on the overlap of the initial wavefunction with the possible steady states and can thus vary. We will discuss this situation in more detail below using the example of two fermions on two sites where almost analytical solutions are found. The occurrence of this entire subspace of steady states induces a very interesting long time dynamics. However, in this work we put the emphasis on the short time dynamics which is more relevant to current experiments, and we postpone further discussions on the long time dynamics to future works.

### III. METHODS

#### A. Eigenvalues and eigenstates for the master equation

The evolution equation (2) is a linear with respect to the density matrix. It can thus be rewritten in the matrix form

$$\partial_t \rho = M \rho. \quad (11)$$

Here  $\rho$  is reordered as a vector and the elements of the matrix  $M$  are chosen to be identified with the right-hand side of the master equation. Using this matrix form is advantageous as the time evolution of an initial density vector  $\rho(t=0)$  is then related to the (complex) eigenvalues  $\lambda_i$  and right eigenvectors  $v_i$  of the non-Hermitian matrix  $M$ , i.e.

$$\rho(t) = \sum_i c_i e^{t\lambda_i} v_i. \quad (12)$$

The weights  $c_i$  are chosen such that the initial state can be represented as  $\rho(t=0) = \sum_i c_i v_i$ . One directly sees from this expression, that the real and imaginary parts of the eigenvalues lead to very different dynamics with time  $t$ . Whereas the imaginary part leads to an oscillatory behavior, a real negative contribution of the eigenvalues leads to an exponential decay. Due to these exponential decays, only the states having null real parts will survive at long times and can potentially be steady states.

##### 1. Application to a system of two fermions on two sites

In this subsection, we consider the simplified problem of two fermions, one with spin up and one with spin down, on two sites. This problem is, to a certain extent, treatable analytically and can already provide a lot of insight

into the interplay of the hopping, interaction and dissipative terms. We will see in the discussion of the results in Sec. IV that the main dynamical effects occurring on two sites are recovered in the extended system. For this system of two sites, we choose the Fock basis ( $|\uparrow\downarrow, 0\rangle$ ,  $|0, \uparrow\downarrow\rangle$ ,  $|\uparrow, \downarrow\rangle$ ,  $|\downarrow, \uparrow\rangle$ ). Within this basis the Hamiltonian is represented as

$$H = \begin{pmatrix} U & 0 & -J & J \\ 0 & U & -J & J \\ -J & -J & 0 & 0 \\ J & J & 0 & 0 \end{pmatrix} \quad (13)$$

and its ground state is given by

$$|GS\rangle = \frac{1}{A_1} \begin{pmatrix} -4J \\ -4J \\ -U - \sqrt{16J^2 + U^2} \\ U + \sqrt{16J^2 + U^2} \end{pmatrix} \quad (14)$$

with  $A_1 = \frac{1}{\sqrt{2(U + \sqrt{16J^2 + U^2})^2 + 32J^2}}$ . The master equation can be understood as 16 coupled differential equations and the density matrix as a vector with 16 entries. Even though this system is still quite complex, a lot of information can be extracted by diagonalizing the matrix  $M$ . This can typically not be fully performed analytically, but approximate analytical expressions are obtained for the dominating eigenvalues. In the following sections, we analyze the effect of the two aforementioned quantum jump operators.

##### 2. Solutions for case (i): dissipative coupling to the local density

In the case of two fermions on two sites where the effective dissipative coupling is to the local density, the dissipator is described by

$$\mathcal{D}_n(\rho) = -\gamma \begin{pmatrix} 0 & 2\rho_{12} & \rho_{13} & \rho_{14} \\ 2\rho_{21} & 0 & \rho_{23} & \rho_{24} \\ \rho_{31} & \rho_{32} & 0 & 2\rho_{34} \\ \rho_{41} & \rho_{42} & 2\rho_{43} & 0 \end{pmatrix} \quad (15)$$

and the eigenvalues can be determined analytically. As we are mainly interested in analyzing time evolutions which begin from the ground state of the Hamiltonian, we restrict our discussion to eigenmodes having an overlap with this ground state. The relevant eigenvalues and

eigenstates are thus

$$\lambda_{n,0} = 0, \quad v_{n,0} = \frac{1}{4} \begin{pmatrix} 1 & 0 & 0 & 0 \\ 0 & 1 & 0 & 0 \\ 0 & 0 & 1 & 0 \\ 0 & 0 & 0 & 1 \end{pmatrix}, \quad (16)$$

$$\lambda_{n,1} = -2\gamma, \quad v_{n,1} = \frac{1}{2} \begin{pmatrix} 0 & -1 & 0 & 0 \\ -1 & 0 & 0 & 0 \\ 0 & 0 & 0 & 1 \\ 0 & 0 & 1 & 0 \end{pmatrix}, \quad (17)$$

$$\lambda_{n,2} = -\gamma - \frac{1}{\sqrt{2}} \sqrt{-16 \left(\frac{J}{\hbar}\right)^2 + \gamma^2 - \left(\frac{U}{\hbar}\right)^2} - A, \quad (18)$$

$$\lambda_{n,3} = -\gamma + \frac{1}{\sqrt{2}} \sqrt{-16 \left(\frac{J}{\hbar}\right)^2 + \gamma^2 - \left(\frac{U}{\hbar}\right)^2} - A, \quad (19)$$

$$\lambda_{n,4} = -\gamma - \frac{1}{\sqrt{2}} \sqrt{-16 \left(\frac{J}{\hbar}\right)^2 + \gamma^2 - \left(\frac{U}{\hbar}\right)^2} + A, \quad (20)$$

$$\lambda_{n,Zeno} = -\gamma + \frac{1}{\sqrt{2}} \sqrt{-16 \left(\frac{J}{\hbar}\right)^2 + \gamma^2 - \left(\frac{U}{\hbar}\right)^2} + A, \quad (21)$$

with  $A = \sqrt{-64\gamma^2 \left(\frac{J}{\hbar}\right)^2 + \left[16 \left(\frac{J}{\hbar}\right)^2 + \gamma^2 + \left(\frac{U}{\hbar}\right)^2\right]^2}$ . Only the eigenvectors corresponding to the first and second eigenvalues have an easy analytical form and have been presented above (in matrix form). The eigenvalue  $\lambda_{n,0}$  is the only one to be null (for  $J, U, \gamma \neq 0$ ) which means that the corresponding density matrix  $v_{n,0}$ , proportional to the identity, is the only asymptotic long-time state of the system. As the identity density matrix corresponds to the infinite temperature state or the totally mixed state of the system, the combined effect of the dissipation and of the Hamiltonian evolution is to heat up the system towards the infinite temperature state. In contrast, the state corresponding to eigenvalue  $\lambda_{n,1}$  decays exponentially with a rate  $2\gamma$ . In turn, the form of the corresponding eigenstate  $v_{n,1}$  implies that the coherence between the doubly occupied states  $|\uparrow\downarrow, 0\rangle$  and  $|0, \uparrow\downarrow\rangle$  and between the states  $|\uparrow, \downarrow\rangle$  and  $|\downarrow, \uparrow\rangle$  is fragile and decays exponentially.

The eigenvalues  $\lambda_{n,2}$  and  $\lambda_{n,3}$  have an imaginary part for all  $\frac{U}{J} > 0$  and  $\frac{\hbar\gamma}{J} \geq 0$  which is, at large values of the interaction strength, proportional to  $U$ . While the imaginary parts cause oscillations, in the region where the overlap of the ground state with these states is maximal, the characteristic damping time,  $\tau_{\text{damp}} = \frac{1}{|\text{Re}(\lambda_{n,2})|}$ , is much shorter than an oscillation period given by  $T = \frac{2\pi}{|\text{Im}(\lambda_{n,2})|}$ . As a consequence, in this regime the oscillations are overdamped. In contrast, the eigenvalues  $\lambda_{n,4}$  and  $\lambda_{n,Zeno}$  are real for all  $\frac{U}{J} \geq 0$  and  $\frac{\hbar\gamma}{J} \geq 0$ . Therefore, the corresponding density matrices will only show

a simple exponential decay. For small hopping elements  $J \ll U, \hbar\gamma$ , the eigenvalues can be well described by

$$\lambda_{n,4} = -2\gamma,$$

and

$$\lambda_{n,Zeno} = -\frac{8\gamma J^2}{(\hbar\gamma)^2 + U^2}.$$

The density matrices corresponding to  $\lambda_{n,4}$  will thus decay rapidly with a decay rate  $2\gamma$ . In contrast, the eigenvalue  $\lambda_{n,Zeno}$  has only a contribution quadratic in the hopping element, and consequently the corresponding density matrix decays very slowly. In particular, for large dissipative coupling the decay rate is approximately given by  $-\frac{8J^2}{\hbar^2\gamma}$  which *decreases* with increasing dissipative coupling  $\gamma$ . This counterintuitive phenomenon is known as the Zeno effect and its origin will be discussed further in section III C. For  $U \gg \hbar\gamma$ , the decay rate is approximated by  $-\frac{8\gamma J^2}{U^2}$ , this effect is known for bosonic systems as interaction impeding effect [11, 12, 18]. A similar slow time-scale arises in the presence of atom losses and has been named non-linear Zeno effect [13–15].

### 3. Solutions for case (ii): dissipative coupling to the local double occupancy

For the coupling to the local double occupancy, the dissipator can be written in the form

$$\mathcal{D}_d(\rho) = -\frac{\gamma}{2} \begin{pmatrix} 0 & 2\rho_{12} & \rho_{13} & \rho_{14} \\ 2\rho_{21} & 0 & \rho_{23} & \rho_{24} \\ \rho_{31} & \rho_{32} & 0 & 0 \\ \rho_{41} & \rho_{42} & 0 & 0 \end{pmatrix}. \quad (22)$$

While determining analytically the full eigensystem for the corresponding evolution equation is very involved, valuable information can already be obtained by considering a few important eigenvalues. Comparing this system to the previous case where the dissipative coupling was through the local density, one important difference is the occurrence of *two* eigenvalues with zero values:

$$\lambda_{d,0} = 0, \quad v_{d,0} = \frac{1}{4} \begin{pmatrix} 1 & 0 & 0 & 0 \\ 0 & 1 & 0 & 0 \\ 0 & 0 & 1 & 0 \\ 0 & 0 & 0 & 1 \end{pmatrix}, \quad (23)$$

$$\lambda'_{d,0} = 0, \quad v'_{d,0} = \frac{1}{2} \begin{pmatrix} 0 & 0 & 0 & 0 \\ 0 & 0 & 0 & 0 \\ 0 & 0 & 1 & 1 \\ 0 & 0 & 1 & 1 \end{pmatrix}. \quad (24)$$

This observation implies that the steady state is not unique anymore, but formed from a combination of these two eigenstates. This situation occurs as the dissipation does not act on singly occupied sites. Therefore, any state in which no doubly occupied sites are present, and

which is additionally an eigenstate of the kinetic part of the Hamiltonian, is stable. As a consequence a coherence between singly occupied states, present in the initial state, survives in the long-time limit. In addition to the steady state values, four other eigenvalues also play an important role if the initial state is the ground state of the Hamiltonian. These are the roots of the polynomial equation in  $\lambda$

$$24\gamma^2 \left(\frac{J}{\hbar}\right)^2 + \left[ \gamma^3 + 80\gamma \left(\frac{J}{\hbar}\right)^2 + 4\gamma \left(\frac{U}{\hbar}\right)^2 \right] \lambda + \left[ 5\gamma^2 + 64 \left(\frac{J}{\hbar}\right)^2 + 4 \left(\frac{U}{\hbar}\right)^2 \right] \lambda^2 + 8\gamma\lambda^3 + 4\lambda^4 = 0. \quad (25)$$

In the limit of  $J \ll \hbar\gamma$ ,  $U$  the corresponding four eigenvalues become

$$\lambda_{d,1} = -\gamma, \quad (26)$$

$$\lambda_{d,2} = -\frac{\gamma}{2} - i\frac{U}{\hbar}, \quad (27)$$

$$\lambda_{d,3} = -\frac{\gamma}{2} + i\frac{U}{\hbar}, \quad (28)$$

$$\lambda_{d,\text{Zeno}} = -\frac{24\gamma J^2}{(\hbar\gamma)^2 + 4U^2}. \quad (29)$$

$$(30)$$

The slowest decay rate is given by the eigenvalue  $\lambda_{d,\text{Zeno}}$ . Similarly to  $\lambda_{n,\text{Zeno}}$  for the case of the coupling to the local density,  $\lambda_{d,\text{Zeno}}$  presents both the ‘‘Zeno’’-behavior proportional to  $\frac{J^2}{\hbar^2\gamma}$  for large  $\gamma$ , and an interaction impeding, proportional to  $\frac{\gamma J^2}{U^2}$  for strong interaction  $U$ . It is interesting to note that the transition to the interaction impeding regime is occurring at smaller values of  $U$  compared to  $\hbar\gamma$  than for  $\lambda_{n,\text{Zeno}}$ . Moreover, when the initial state is the ground state of the Hamiltonian, the amplitude of the overlap with this slowly decaying state increases with increasing  $U$ . In this regime of large interaction, the slow decaying ‘‘eigenmatrix’’ is proportional, up to zeroth order in the hopping, to

$$v_{d,\text{Zeno}} = \frac{1}{2} \begin{pmatrix} -1 & 0 & 0 & 0 \\ 0 & -1 & 0 & 0 \\ 0 & 0 & 1 & -1 \\ 0 & 0 & -1 & 1 \end{pmatrix}. \quad (31)$$

This state is clearly invariant under the action of the dissipator  $\mathcal{D}_d$ , Eq. (22), but is connected via the kinetic term to states which are not invariant under the action of the dissipator. Thus, even though the dissipator does not directly act on state  $v_{d,\text{Zeno}}$ , this state decays due to the interplay of the Hamiltonian and dissipative terms. In contrast, due to a direct coupling to the dissipation, the other relevant eigenvalues correspond to much faster decay rates of the order of  $\gamma$ . Additionally, the imaginary parts of  $\lambda_{d,2}$  and  $\lambda_{d,3}$  induce oscillations (present for large interaction strength), the frequency of which is approximately linear in  $U/\hbar$ .

## B. Dissipative dynamics within a slave-spin representation approach

### 1. Definition of the slave-spin representation

We explain here how the slave-spin representation of fermionic operators, first developed to study the equilibrium physics of multi-orbital Hubbard models [23], can be successfully applied to explore the short-time dynamics of dissipative fermionic systems. As for any slave-field representations, the slave-spin approach relies on enlarging the Hilbert space and then imposing a local constraint to eliminate unphysical states. The objective of this approach is to choose the auxiliary states in a way which will allow one to handle the model with greater ease. Applying the constraint on average effectively corresponds to treating the system within the mean-field approximation.

The fermionic slave-spin representation was developed following the realization that the two possible occupancies of a spinless fermion on a given site,  $n_c = 0$  and  $n_c = 1$ , can be considered as the two possible states of a spin- $\frac{1}{2}$  variable,  $S^z = -\frac{1}{2}$  and  $S^z = \frac{1}{2}$ , a mapping widely used to represent hard-core bosons. Here the label ‘‘ $c$ ’’ denotes the physical fermion. In the fermionic context, where anticommutation properties need to be maintained, one also introduces an auxiliary fermionic field,  $f$ , and the local constraint  $S^z + \frac{1}{2} = f^\dagger f$  which, together, translate into a faithful representation of the Hilbert space:

$$\begin{aligned} |n_c = 0\rangle &= |n_f = 0, S^z = -\frac{1}{2}\rangle, \\ |n_c = 1\rangle &= |n_f = 1, S^z = +\frac{1}{2}\rangle. \end{aligned} \quad (32)$$

This representation is often useful as it allows one to choose the auxiliary fermionic sector in such a way that it consists solely of non-interacting terms. The more intricate interaction terms are all described using auxiliary spins (in other words, in the charge sector) allowing for a more effective treatment.

One can correctly wonder why we chose, among the plethora of slave-field representations developed over the years for Hamiltonian systems, to extend the slave-spin representation method to dissipative systems.

It is known that different slave-variable representations lead to different mean-field theories, and that, generally, the quality of a given mean-field treatment can be improved by adapting the slave fields to a system specificities. For equilibrium problems, one usually tries to find the right balance between the simplicity of the representation, the number of unphysical states introduced, and the possibility of an analytical treatment for the resulting mean-field theory. In the case of time-dependent problems, the optimal conditions are, to the best of our knowledge, not as well known. From our experience, it appears that a good description of the system dynamics can be achieved if the Hilbert space of the relevant sector

(charge or spin) is of the correct physical size even when the constraint is only applied on average. When the size of the sector is enlarged, we noticed that the presence of spurious states usually lead to unphysical interference effects. For example, we found that the celebrated slave-rotor approach [31] cannot be used to study the dynamics of the charge sector because, at the mean-field level, the presence of unphysical states leads to catastrophic interference effects and thus gives unphysical evolutions.

Within the slave-spin representation, there is a certain freedom in choosing the appropriate representation for the physical fermions. As we consider here a half-filled system, we choose the representation

$$\begin{aligned} c_{\mathbf{r},\sigma}^\dagger &\rightarrow 2S_{\mathbf{r},\sigma}^x f_{\mathbf{r},\sigma}^\dagger, \\ c_{\mathbf{r},\sigma} &\rightarrow 2S_{\mathbf{r},\sigma}^x f_{\mathbf{r},\sigma}, \end{aligned} \quad (33)$$

which is correct on the physical Hilbert space. This choice ensures that the single particle spectral weight  $Z$  (the amplitude corresponding to a single particle state) remains equal to one for  $U = 0$  even when further mean-field approximations are made [31]. With this choice, the Fermi-Hubbard Hamiltonian takes the form

$$\begin{aligned} H = & -4J \sum_{\mathbf{r},\mathbf{r}'(\mathbf{r}),\sigma} f_{\mathbf{r}\sigma}^\dagger f_{\mathbf{r}'\sigma} S_{\mathbf{r}\sigma}^x S_{\mathbf{r}'\sigma}^x + \frac{U}{2} \sum_{\mathbf{r}} \left( \sum_{\sigma} S_{\mathbf{r}\sigma}^z \right)^2 \\ & + \theta \sum_{\mathbf{r},\sigma} \left( S_{\mathbf{r}\sigma}^z + \frac{1}{2} - f_{\mathbf{r}\sigma}^\dagger f_{\mathbf{r}\sigma} \right). \end{aligned} \quad (34)$$

Here the last term enforces the local constraint on average using the Lagrange multiplier  $\theta$ . As we restrict ourselves to the situation where the system is half-filled, we can set  $\theta = 0$ . The Lagrange multiplier term then disappears all together.

One can further recast the dissipator within the slave-spin representation. However, this rewriting is not unique as the jump operators can be written using either the auxiliary fermionic or spin operators. The most appropriate choice often depends on the tractability of the resulting equation of motion. We choose here to recast the dissipator,  $\mathcal{D}(\rho)$ , using exclusively the auxiliary spin operators. When the dissipation couples to the local density, the jump operator is rewritten as  $j_{\mathbf{r}\sigma} = n_{\mathbf{r}\sigma} \rightarrow S_{\mathbf{r}\sigma}^z + \frac{1}{2}$  and the dissipator adopts the simple form

$$\mathcal{D}_n^s(\rho) = \gamma \sum_{\mathbf{r},\sigma} \left( S_{\mathbf{r}\sigma}^z \rho S_{\mathbf{r}\sigma}^z - \frac{1}{4} \rho \right). \quad (35)$$

While for coupling to the double occupancy density, the jump operator is recast as  $j_{\mathbf{r}\sigma} = \frac{1}{\sqrt{2}} n_{\mathbf{r}\uparrow} n_{\mathbf{r}\downarrow} \rightarrow \frac{1}{\sqrt{2}} (S_{\mathbf{r}\uparrow}^z S_{\mathbf{r}\downarrow}^z + \frac{1}{2} S_{\mathbf{r}\uparrow}^z + \frac{1}{2} S_{\mathbf{r}\downarrow}^z + \frac{1}{4})$ . In this case, we denote the dissipator as  $D_d^s(\rho)$ .

## 2. The Lindblad equation within the slave-spin representation

Now that we have recast the Fermi-Hubbard Hamiltonian and the dissipator within the slave-spin representa-

tion, we can find the corresponding Lindblad equation. We assume here that the density matrix representing the system is a direct product of the spin and fermionic auxiliary spaces, i.e.  $\rho = \rho^s \otimes \rho^f$ . This assumption is often justified but implies that the charge and spin sectors are only minimally coupled. This procedure can be further generalized, if one considers the general decomposition of a density matrix into the weighted sum of several such products and evolve each term separately as permitted by the linear character of the evolution equations.

Using this choice for the density matrix, the Lindblad equation takes the form

$$\begin{aligned} \dot{\rho}^s \otimes \rho^f + \rho^s \otimes \dot{\rho}^f = & \quad (36) \\ -\frac{i}{\hbar} \left[ -4J \sum_{\mathbf{r},\mathbf{r}'(\mathbf{r}),\sigma} f_{\mathbf{r}\sigma}^\dagger f_{\mathbf{r}'\sigma} S_{\mathbf{r}\sigma}^x S_{\mathbf{r}'\sigma}^x \right. & \\ \left. + \frac{U}{2} \sum_{\mathbf{r}} \left( \sum_{\sigma} S_{\mathbf{r}\sigma}^z \right)^2, \rho^s \otimes \rho^f \right] + D^s(\rho^s) \otimes \rho^f. & \end{aligned}$$

Taking partial traces over the fermionic and spin auxiliary spaces, we obtain two coupled differential equations. The evolution of the auxiliary spin space (the charge sector) is described by the equation

$$\begin{aligned} \dot{\rho}^s = & -\frac{i}{\hbar} \left[ -4J \sum_{\mathbf{r},\mathbf{r}'(\mathbf{r}),\sigma} \text{Tr}_f (f_{\mathbf{r}\sigma}^\dagger f_{\mathbf{r}'\sigma}) S_{\mathbf{r}\sigma}^x S_{\mathbf{r}'\sigma}^x \right. \\ & \left. + \frac{U}{2} \sum_{\mathbf{r}} \left( \sum_{\sigma} S_{\mathbf{r}\sigma}^z \right)^2, \rho^s \right] + D^s(\rho^s). \end{aligned} \quad (37)$$

While the evolution of the fermionic part of the density matrix (the spin sector) is given by the differential equation

$$\dot{\rho}^f = -\frac{i}{\hbar} \left[ -4J \sum_{\mathbf{r},\mathbf{r}'(\mathbf{r}),\sigma} \text{Tr}_s (S_{\mathbf{r}\sigma}^x S_{\mathbf{r}'\sigma}^x) f_{\mathbf{r}\sigma}^\dagger f_{\mathbf{r}'\sigma}, \rho^f \right]. \quad (38)$$

To summarize our result up to this point, we now have two coupled mean-field Lindblad equations describing the evolution of the spin and charge sectors of a dissipative half-filled fermionic system. Our main approximation was to apply only on average the constraint ensuring the correct dimensionality of the system Hilbert space.

## 3. Further mean-field decoupling

To make further progress, we perform a mean-field decoupling of the charge sector which corresponds to rewriting the density matrix as a direct product over all sites:  $\rho^s = \bigotimes_{\mathbf{r}} \rho_{\mathbf{r}}^s$ . Additionally, as we are dealing with a translationally invariant system, we assume that all  $\rho_{\mathbf{r}}^s$  are equal and denote the local density matrix as  $\tilde{\rho}^s$ . Under

this simplification, the Lindblad equation for the auxiliary fermions can be brought to a diagonal form in momentum space:

$$\dot{\rho}^f = -\frac{i}{\hbar} \left[ \sum_{\mathbf{k}\sigma} Z_\sigma(t) \epsilon_{\mathbf{k}} n_{\mathbf{k}\sigma}, \rho^f \right] \quad (39)$$

where  $Z_\sigma(t)$ , the charge spectral weight, is given by

$$Z_\sigma(t) = 4 (\text{Tr}_s(S_\sigma^x \tilde{\rho}^s))^2 = 4 \langle S_\sigma^x \rangle^2 \quad (40)$$

with  $\epsilon_{\mathbf{k}} = -J \sum_{\mathbf{r}'(\mathbf{r})} e^{i \mathbf{k} \cdot (\mathbf{r} - \mathbf{r}')}$ . Interestingly, one can show that when the evolution begins from the ground state of the mean-field Fermi-Hubbard model, which corresponds, for the auxiliary fermions, to the Fermi sea, the density matrix  $\rho^f$  is time independent.

In contrast, the evolution of the charge sector is much more involved as the interaction and dissipative terms have been exclusively rewritten using auxiliary spins. At the mean-field level, and under the assumption of translational invariance, the evolution equation for this sector reads

$$\begin{aligned} \dot{\tilde{\rho}}^s = & -\frac{i}{\hbar} \left[ -J_{\text{eff}} \sum_{\sigma} \langle S_\sigma^x \rangle S_\sigma^x + \frac{U}{2} \left( \sum_{\sigma} S_\sigma^z \right)^2, \tilde{\rho}^s \right] \\ & + D_{\text{loc}}^s(\tilde{\rho}^s) \end{aligned} \quad (41)$$

where the effective time-independent auxiliary spin coupling (independent of  $\sigma$  at half-filling) is

$$\begin{aligned} J_{\text{eff}} = J_{\text{eff}}^\sigma &= -\frac{8}{\Omega} \sum_{\mathbf{k}} \epsilon_{\mathbf{k}} \text{Tr}_f(n_{\mathbf{k}\sigma} \rho^f) \\ &= -\frac{8}{\Omega} \sum_{\mathbf{k}} \epsilon_{\mathbf{k}} \langle n_{\mathbf{k}\sigma} \rangle \end{aligned}$$

with  $\Omega$  the number of sites.  $D_{\text{loc}}^s(\tilde{\rho}^s)$  is the local dissipator defined as

$$D_{\text{loc}}^s(\tilde{\rho}^s) = \gamma \sum_{\sigma} \left( j_\sigma \tilde{\rho}^s j_\sigma - \frac{1}{2} j_\sigma^2 \tilde{\rho}^s - \frac{1}{2} \tilde{\rho}^s j_\sigma^2 \right).$$

Consequently, to understand the evolution of the charge under both dissipative and interaction effects, we solve Eq. (41) to find  $\tilde{\rho}^s(t)$ . Alternatively, we can consider directly the evolution of any observable of the charge sector,  $O$ , using the Heisenberg equation [27]

$$\begin{aligned} \frac{d}{dt} \langle O \rangle = & \left\langle i \left[ -J_{\text{eff}} \sum_{\sigma} \langle S_\sigma^x \rangle S_\sigma^x + \frac{U}{2} \left( \sum_{\sigma} S_\sigma^z \right)^2, O \right] \right\rangle \\ & + \langle D_{\text{loc}}^s(O) \rangle \end{aligned} \quad (42)$$

as  $\langle O(t) \rangle = \text{Tr}_s(O \tilde{\rho}^s(t))$ . As Eq. (42) provides us with a more intuitive understanding of the physics at play, we will predominantly use this alternative form in the following sections to study the evolution of the charge sector.

#### 4. Mean-field ground state in the charge sector

As mentioned previously, we want to evolve the system from its ground state that it is decoupled from the dissipative environment. We therefore want to determine the ground state of the mean-field Hamiltonian

$$H = -J_{\text{eff}} \sum_{\sigma} \langle S_\sigma^x \rangle S_\sigma^x + \frac{U}{2} \left( \sum_{\sigma} S_\sigma^z \right)^2. \quad (43)$$

As at half-filling  $\langle S_\sigma^u \rangle = \langle S_\sigma^v \rangle$  and  $\langle S_\sigma^u S_\sigma^v \rangle = \langle S_\sigma^u S_\sigma^v \rangle$  for  $u, v \in \{x, y, z\}$ , we identify the ground state by requiring that

$$\langle \Psi(J_{\text{eff}}, U, \langle S_\uparrow^x \rangle) | S_\uparrow^x | \Psi(J_{\text{eff}}, U, \langle S_\uparrow^x \rangle) \rangle = \langle S_\uparrow^x \rangle \quad (44)$$

where  $|\Psi(J_{\text{eff}}, U, \langle S_\uparrow^x \rangle)\rangle$  is the ground state wavefunction obtained by diagonalizing the mean-field Hamiltonian given by Eq. (43) while holding  $\langle S_\uparrow^x \rangle$  fixed. Using this self-consistent approach, we find that in the ground state

$$\langle S_\uparrow^x \rangle_{\text{gs}} = \frac{1}{4} \sqrt{4 - \left( \frac{U}{J_{\text{eff}}} \right)^2} \quad (45)$$

in the range  $0 \leq U \leq 2J_{\text{eff}}$ , and 0 for  $U > 2J_{\text{eff}}$ . In the first range, we also identify that

$$\begin{aligned} \langle S_\uparrow^x S_\downarrow^x \rangle_{\text{gs}} &= \frac{1}{4}, \\ \langle S_\uparrow^y S_\downarrow^y \rangle_{\text{gs}} &= \frac{U}{8J_{\text{eff}}}, \\ \langle S_\uparrow^z S_\downarrow^z \rangle_{\text{gs}} &= -\frac{U}{8J_{\text{eff}}}, \end{aligned}$$

while  $\langle S_\uparrow^y \rangle$ ,  $\langle S_\uparrow^z \rangle$ ,  $\langle S_\uparrow^x S_\downarrow^y \rangle$ ,  $\langle S_\uparrow^x S_\downarrow^z \rangle$ , and  $\langle S_\uparrow^y S_\downarrow^z \rangle$  are zero in the ground state. Consequently, within this mean-field approximation, we obtain that a metallic phase with spectral weight  $Z_\sigma = 1 - \left( \frac{U}{2J_{\text{eff}}} \right)^2$  exists for  $0 \leq U \leq 2J_{\text{eff}}$ . As expected, our choice of representation for the physical fermions, Eq. (33), captures correctly that  $Z = 1$  at  $U = 0$ . This simple mean-field model also predicts correctly that the double occupation,  $\langle n_\uparrow n_\downarrow \rangle$ , is  $\frac{1}{4}$  at  $U = 0$  and zero when the system becomes insulating and that the local density,  $\langle n_\uparrow \rangle + \langle n_\downarrow \rangle$ , is one for all  $U$ . These findings are in agreement with results obtained in previous studies based on the slave-spin method [23, 32].

#### 5. Case (i): Dissipative coupling to the local density

We can now use our newly developed mean-field formalism to study the evolution of an interacting fermionic system dissipatively coupled to its environment through the local density, i.e. for the jump operator  $j_{\mathbf{r},\sigma} = n_{\mathbf{r},\sigma}$ . We consider here a situation where the fermionic system is initially metallic (low interaction  $U$ ) and isolated from its environment. As we want to understand how

the charge spectral weight evolves under the influence of dissipative effects, we need to consider the evolution of  $\langle S_\sigma^x \rangle$ . We identify a set of four coupled differential equations that needs to be solved together to uncover the evolution of the spectral weight  $Z_\sigma$ :

$$\frac{d}{dt} \langle S_\uparrow^x \rangle = -\frac{\gamma}{2} \langle S_\uparrow^x \rangle - \frac{U}{\hbar} \langle S_\uparrow^y S_\downarrow^z \rangle, \quad (46)$$

$$\frac{d}{dt} \langle S_\uparrow^z S_\downarrow^z \rangle = -2 \frac{J_{\text{eff}}}{\hbar} \langle S_\uparrow^x \rangle \langle S_\uparrow^y S_\downarrow^z \rangle, \quad (47)$$

$$\frac{d}{dt} \langle S_\uparrow^y S_\downarrow^y \rangle = -\gamma \langle S_\uparrow^y S_\downarrow^y \rangle + 2 \frac{J_{\text{eff}}}{\hbar} \langle S_\uparrow^x \rangle \langle S_\uparrow^y S_\downarrow^z \rangle, \quad (48)$$

$$\begin{aligned} \frac{d}{dt} \langle S_\uparrow^y S_\downarrow^z \rangle &= -\frac{\gamma}{2} \langle S_\uparrow^y S_\downarrow^z \rangle + \frac{U}{4\hbar} \langle S_\uparrow^x \rangle \\ &+ \frac{J_{\text{eff}}}{\hbar} \langle S_\uparrow^x \rangle \left( \langle S_\uparrow^z S_\downarrow^z \rangle - \langle S_\uparrow^y S_\downarrow^y \rangle \right). \end{aligned} \quad (49)$$

In the following, we discuss the solution of this set of equations for various instantaneous quenches where the metallic state is quenched (at  $t = 0$ ) to analytically solvable limits:

*a. Instantaneous quench to  $U = 0$ .* When the metallic system is quenched to the non-interacting limit, the equation for  $\langle S_\uparrow^x \rangle$  is closed and is written as

$$\frac{d}{dt} \langle S_\uparrow^x \rangle = -\frac{\gamma}{2} \langle S_\uparrow^x \rangle, \quad (50)$$

which has for solution

$$\langle S_\uparrow^x(t) \rangle = \langle S_\uparrow^x \rangle_{t=0} e^{-\frac{\gamma}{2}t}. \quad (51)$$

In this limit, the charge spectral weight,  $Z(t) = 4 \langle S_\uparrow^x(t) \rangle^2$ , decays exponentially fast with rate  $\gamma$ .

*b. Instantaneous quench to  $J_{\text{eff}} = 0$ .* When the metallic system is quenched to a limit where the lattice sites decouple, considering the two following equations is sufficient:

$$\begin{aligned} \frac{d}{dt} \langle S_\uparrow^x \rangle &= -\frac{\gamma}{2} \langle S_\uparrow^x \rangle - \frac{U}{\hbar} \langle S_\uparrow^y S_\downarrow^z \rangle, \\ \frac{d}{dt} \langle S_\uparrow^y S_\downarrow^z \rangle &= -\frac{\gamma}{2} \langle S_\uparrow^y S_\downarrow^z \rangle + \frac{U}{4\hbar} \langle S_\uparrow^x \rangle. \end{aligned} \quad (52)$$

These equations have for solution

$$\begin{aligned} \langle S_\uparrow^x(t) \rangle &= e^{-\frac{\gamma}{2}t} \left[ B_1 \cos\left(\frac{U}{2\hbar}t\right) - 2B_2 \sin\left(\frac{U}{2\hbar}t\right) \right], \\ \langle S_\uparrow^y S_\downarrow^z(t) \rangle &= e^{-\frac{\gamma}{2}t} \left[ B_2 \cos\left(\frac{U}{2\hbar}t\right) + \frac{B_1}{2} \sin\left(\frac{U}{2\hbar}t\right) \right]. \end{aligned} \quad (53)$$

As the evolution begins from the metallic state, we obtain that  $B_2 = 0$  and  $B_1 = \frac{1}{4} \sqrt{4 - \left(\frac{U}{J_{\text{eff}}}\right)^2}$ . This result indicates that  $\langle S_\uparrow^x(t) \rangle$  decays exponentially with rate  $\gamma/2$ , but that this decay is dressed with oscillations of period  $T_p = 4\pi\hbar/U$ .

## 6. Case (ii): Dissipative coupling to the double occupancy

We also explore the evolution of an interacting fermionic system dissipatively coupled to its environment through the local double occupancy, i.e. for the jump operator  $j_{\mathbf{r}} = \frac{1}{\sqrt{2}} n_{\mathbf{r},\uparrow} n_{\mathbf{r},\downarrow}$ . We consider once again an initial situation where the fermionic system is half-filled, metallic and isolated from its environment. In this case, to understand the behavior of the charge spectral weight, one needs to solve the following set of equations:

$$\frac{d}{dt} \langle S_\uparrow^x \rangle = -\frac{U}{\hbar} \langle S_\uparrow^y S_\downarrow^z \rangle - \frac{\gamma}{2} \left( \langle S_\uparrow^x S_\downarrow^x \rangle + \frac{1}{2} \langle S_\uparrow^x \rangle \right), \quad (54)$$

$$\begin{aligned} \frac{d}{dt} \langle S_\uparrow^y S_\downarrow^z \rangle &= \frac{U}{4\hbar} \langle S_\uparrow^x \rangle + \frac{J_{\text{eff}}}{\hbar} \langle S_\uparrow^x \rangle \left( \langle S_\uparrow^z S_\downarrow^z \rangle - \langle S_\uparrow^y S_\downarrow^y \rangle \right) \\ &- \frac{\gamma}{4} \left( \langle S_\uparrow^y S_\downarrow^z \rangle + \frac{1}{2} \langle S_\uparrow^y \rangle \right), \end{aligned} \quad (55)$$

$$\begin{aligned} \frac{d}{dt} \langle S_\uparrow^x S_\downarrow^z \rangle &= -\frac{U}{4\hbar} \langle S_\uparrow^y \rangle - \frac{J_{\text{eff}}}{\hbar} \langle S_\uparrow^x \rangle \langle S_\uparrow^x S_\downarrow^y \rangle \\ &- \frac{\gamma}{4} \left( \langle S_\uparrow^x S_\downarrow^z \rangle + \frac{1}{2} \langle S_\uparrow^x \rangle \right), \end{aligned} \quad (56)$$

$$\begin{aligned} \frac{d}{dt} \langle S_\uparrow^y \rangle &= \frac{J_{\text{eff}}}{\hbar} \langle S_\uparrow^x \rangle \langle S_\uparrow^z \rangle + \frac{U}{\hbar} \langle S_\uparrow^x S_\downarrow^z \rangle \\ &- \frac{\gamma}{2} \left( \langle S_\uparrow^y S_\downarrow^z \rangle + \frac{1}{2} \langle S_\uparrow^y \rangle \right), \end{aligned} \quad (57)$$

$$\frac{d}{dt} \langle S_\uparrow^z \rangle = -\frac{J_{\text{eff}}}{\hbar} \langle S_\uparrow^x \rangle \langle S_\uparrow^y \rangle, \quad (58)$$

$$\frac{d}{dt} \langle S_\uparrow^x S_\downarrow^x \rangle = \frac{\gamma}{4} \left( \langle S_\uparrow^y S_\downarrow^y \rangle - \langle S_\uparrow^x S_\downarrow^x \rangle \right), \quad (59)$$

$$\frac{d}{dt} \langle S_\uparrow^x S_\downarrow^y \rangle = -\frac{\gamma}{2} \langle S_\uparrow^x S_\downarrow^y \rangle + \frac{J_{\text{eff}}}{\hbar} \langle S_\uparrow^x \rangle \langle S_\uparrow^x S_\downarrow^z \rangle, \quad (60)$$

$$\begin{aligned} \frac{d}{dt} \langle S_\uparrow^y S_\downarrow^y \rangle &= -\frac{\gamma}{4} \left( \langle S_\uparrow^y S_\downarrow^y \rangle - \langle S_\uparrow^x S_\downarrow^x \rangle \right) \\ &+ 2 \frac{J_{\text{eff}}}{\hbar} \langle S_\uparrow^x \rangle \langle S_\uparrow^y S_\downarrow^z \rangle, \end{aligned} \quad (61)$$

$$\frac{d}{dt} \langle S_\uparrow^z S_\downarrow^z \rangle = -2 \frac{J_{\text{eff}}}{\hbar} \langle S_\uparrow^x \rangle \langle S_\uparrow^y S_\downarrow^z \rangle. \quad (62)$$

As for the case of the density coupling, we solve these equations numerically to obtain the behavior of  $\langle S_\sigma^x \rangle$  for general combinations of the parameters  $U$ ,  $J_{\text{eff}}$  and  $\gamma$ . We present the results for this general case in a later section. For now we consider the limiting case of an instantaneous quench to the non-interacting limit  $U = 0$ . In this case, one only needs Eqs. (54), (56) and (60) to uncover the evolution of the spectral weight. After a few algebraic manipulations, these three equations can be combined into one to give

$$\begin{aligned} \frac{d^2}{dt^2} \langle S_\uparrow^x \rangle &+ \frac{\gamma}{2} \frac{d}{dt} \langle S_\uparrow^x \rangle + \frac{1}{2} \frac{J_{\text{eff}}^2}{\hbar^2} \langle S_\uparrow^x \rangle^3 \\ &- \langle S_\uparrow^x(0) \rangle^2 \frac{J_{\text{eff}}^2}{2\hbar^2} e^{-\frac{\gamma}{2}t} \langle S_\uparrow^x \rangle = 0 \end{aligned} \quad (63)$$

together with the initial condition

$$\frac{d}{dt} \langle S_\uparrow^x \rangle|_{t=0} = -\frac{\gamma}{2} \left( \langle S_\uparrow^x S_\downarrow^z(0) \rangle + \frac{1}{2} \langle S_\uparrow^x(0) \rangle \right). \quad (64)$$



At long times, we find surprisingly that the solution is given by an algebraic decay following

$$\langle S_{\uparrow}^x(t) \rangle \sim \sqrt{\frac{1}{\gamma t}}. \quad (65)$$

A similar algebraic decay has been seen before for a dissipative coupling to the spin density difference [8] in fermionic systems, in bosonic systems [12, 15, 18] and in spin systems [33]. However, the validity of this result is questionable as this algebraic decay occurs at long times, a regime where the slave-spin approach combined with the mean-field approximation is believed to lack accuracy. Obtaining the same result using an alternative method would be highly valuable.

### C. Adiabatic elimination method

In this section, we discuss how the adiabatic elimination method is applied to study the evolution of strongly-interacting dissipative fermionic systems. Adiabatic elimination is commonly used in quantum optics [25–27] to understand, for example, the interaction of light fields with single atoms. However, in the area of strongly correlated systems, this method has only become popular recently (see for example [4, 6, 8, 12, 18, 34] and references therein). The idea behind adiabatic elimination is to derive an effective description of the *slow* degrees of freedom, by coarse graining the time evolution and taking only virtual transitions to fast modes into account. Therefore, adiabatic elimination describes well the effective slow (long time) dynamics of the system. This approach is complementary to the slave-spin method presented in the previous section as the latter is good, at the mean-field level, to describe the short time dynamics.

We concentrate here on case (i): the dissipative coupling with the local density as the quantum jump operator. The decoherence free subspace of the dissipator  $\mathcal{D}_n$  is given by density matrices which are diagonal in the Fock representation. A density matrix in this decoherence free subspace can be represented by  $\rho = \sum_{\vec{m}} \rho_{\vec{m}}^{\vec{m}} |\vec{m}\rangle \langle \vec{m}|$ . Here the vector  $\vec{m} = (m_1, m_2, m_3, \dots, m_{\Omega})$  denotes a chosen configuration of states. The local states on site  $j = 1, \dots, \Omega$  are denoted by  $m_j = 0, \uparrow, \downarrow$  or  $\uparrow\downarrow$ .  $\rho_{\vec{m}}^{\vec{m}}$  is the weight of the diagonal state: a diagonal element within the Fock representation. Both the unitary evolution, caused by the interaction term, and the dissipative evolution leave the diagonal elements of the density matrix  $\rho$  invariant. In contrast, the action of the dissipator on the off-diagonal terms of a density matrix is proportional to the coupling strength  $\gamma$  and thus induces a decay at a rate proportional to the coupling strength. Therefore, at long times, the dynamics will be dominated by the diagonal terms. In this regime, the evolution is driven by the kinetic term of the Hamiltonian which couples the decoherence free subspace to small and fast decaying

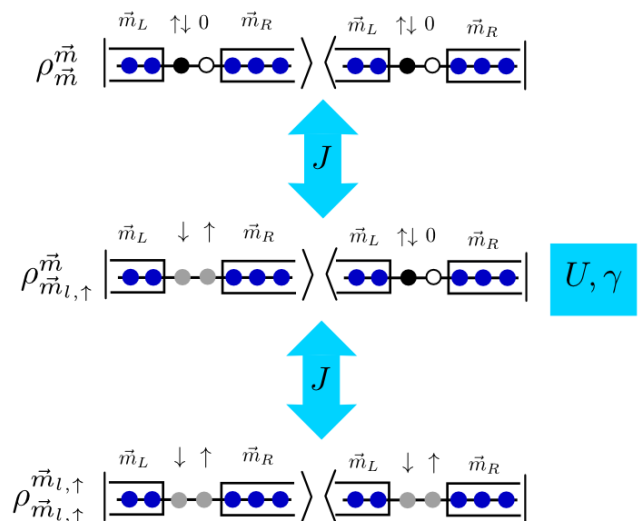


FIG. 1: (Color online): Schematic of the adiabatic elimination treatment. The slow diagonal states  $\rho_{\vec{m}}^{\vec{m}}$  and  $\rho_{\vec{m}_{l,\uparrow}}^{\vec{m}}$  are connected via excitations (arrow  $J$ ) to the fast decaying state  $\rho_{\vec{m}_{l,\uparrow}}^{\vec{m}}$  on which both the interaction,  $U$ , and dissipation,  $\gamma$ , terms can act.

off-diagonal terms (see Fig. 1). Coarse graining the time-scale of the dynamical evolution allows one to describe the system effective slow dynamics using solely diagonal matrices as the connection to the off-diagonal matrices is integrated out. This effective dynamics, which plays out within the decoherence free subspace, can be formulated as a classical master equation for the different diagonal configurations as derived below.

In the following, we will first show an example of how the integration of the fast degrees of freedom is performed in order to obtain the classical master equations. Afterwards, we will perform the mean-field decoupling, and derive an effective equation for the dynamics of the reduced single site density matrix. For notational simplicity we will refer here to a linear chain, however, these results can be easily extended to higher dimensions.

#### 1. Adiabatic elimination of the fast modes

As an illustrative example, we will derive in the following the classical master equations determining the evolution of the weight  $\rho_{\vec{m}}^{\vec{m}}(t)$  corresponding to a configuration of atoms in which the site  $l$  is doubly occupied, i.e.  $m_l = \uparrow\downarrow$ .

Off-diagonal elements are generated starting from the diagonal configuration by the application of a local hopping term, e.g.  $\rho_{\vec{m}_{l,\sigma}}^{\vec{m}} |\vec{m}_{l,\sigma}\rangle \langle \vec{m}| = \left( c_{l+1,\sigma}^\dagger c_{l,\sigma} \rho_{\vec{m}}^{\vec{m}} |\vec{m}\rangle \langle \vec{m}| \right)$  with  $\sigma = \uparrow, \downarrow$ . The action is only non-zero for  $m_{l+1} = 0$  or  $m_{l+1} = \bar{\sigma}$ , where  $\bar{\sigma}$  is the opposite of  $\sigma$ . We will only discuss these cases in the following. The corresponding generated configuration is then given by  $\vec{m}_{l,\sigma} =$

$(\vec{m}_L, m'_{l,\sigma}, m'_{l+1,\sigma}, \vec{m}_R)$  with  $m'_{l,\sigma} = \bar{\sigma}$  and  $m'_{l+1,\sigma} = \sigma$  for  $m_{l+1} = 0$  and  $m'_{l+1,\sigma} = \uparrow\downarrow$  for  $m_{l+1} = \bar{\sigma}$ .  $\vec{m}_L$  and  $\vec{m}_R$  are, respectively, the vector of the configuration of fermions to the left of site  $l$  and to the right of site  $l+1$ . Neglecting small and fast decaying off-diagonal terms, the evolution of  $\rho_{\vec{m}_l,\sigma}^{\vec{m}}$  is given by

$$\begin{aligned} \hbar\partial_t \rho_{\vec{m}_l,\sigma}^{\vec{m}} &= [-\hbar\gamma + iU(1 - n_{l+1,\bar{\sigma}})] \rho_{\vec{m}_l,\sigma}^{\vec{m}} \\ &+ iJ \left( \rho_{\vec{m}}^{\vec{m}} - \rho_{\vec{m}_l,\sigma}^{\vec{m}_l,\sigma} \right), \end{aligned} \quad (66)$$

where  $n_{l+1,\bar{\sigma}}$  is the occupation of the particle with spin  $\bar{\sigma}$  on site  $l+1$  in the configuration  $\vec{m}$ . This equation can be integrated giving [35]

$$\begin{aligned} \rho_{\vec{m}_l,\sigma}^{\vec{m}}(t) &= e^{-(\gamma - iU(1 - n_{l+1,\bar{\sigma}})/\hbar)t} \rho_{\vec{m}_l,\sigma}^{\vec{m}}(0) \\ &+ i(J/\hbar) e^{-(\gamma - iU(1 - n_{l+1,\bar{\sigma}})/\hbar)t} \\ &\times \int_0^t e^{(\gamma - iU(1 - n_{l+1,\bar{\sigma}})/\hbar)\tau} \left( \rho_{\vec{m}}^{\vec{m}}(\tau) - \rho_{\vec{m}_l,\sigma}^{\vec{m}_l,\sigma}(\tau) \right) d\tau. \end{aligned} \quad (67)$$

After an integration by parts and neglecting the fast decaying and dephasing terms, this leads to

$$\rho_{\vec{m}_l,\sigma}^{\vec{m}}(t) = -\frac{J}{U(1 - n_{l+1,\bar{\sigma}}) + i\hbar\gamma} \left( \rho_{\vec{m}}^{\vec{m}}(t) - \rho_{\vec{m}_l,\sigma}^{\vec{m}_l,\sigma}(t) \right). \quad (68)$$

The diagonal density matrices evolution is only connected to these off-diagonal elements thus giving

$$\frac{d}{dt} \rho_{\vec{m}}^{\vec{m}} = \frac{J}{\hbar} \sum_{l,\sigma} \left( i\rho_{\vec{m}_l,\sigma}^{\vec{m}_l,\sigma} + \text{h.c.} \right). \quad (69)$$

Inserting Eq. (68) into Eq. (69), we obtain

$$\frac{d}{dt} \rho_{\vec{m}}^{\vec{m}} = -\sum_{l,\sigma} \frac{J^2\gamma}{(\hbar\gamma)^2 + U^2(1 - n_{l+1,\bar{\sigma}})^2} \left( \rho_{\vec{m}}^{\vec{m}} - \rho_{\vec{m}_l,\sigma}^{\vec{m}_l,\sigma} \right). \quad (70)$$

For the general case, where  $m_l$  and  $m_{l+1}$  can take any value, the evolution equation naturally becomes

$$\frac{d}{dt} \rho_{\vec{m}}^{\vec{m}} = -\sum_{l,\sigma} \frac{J^2\gamma [n_{l+1,\sigma}(1 - n_{l+1,\sigma})]}{(\hbar\gamma)^2 + U^2(n_{l,\bar{\sigma}} - n_{l+1,\bar{\sigma}})^2} \left( \rho_{\vec{m}}^{\vec{m}} - \rho_{\vec{m}_l,\sigma}^{\vec{m}_l,\sigma} \right). \quad (71)$$

We have therefore derived the effective classical master equations describing the evolution of the diagonal elements of the density matrices by integrating out the off-diagonal parts.

## 2. Thermodynamic limit

The set of equations (70) can in principle be solved numerically, i.e. by classical Monte-Carlo methods. However, as a large number of degrees of freedom is still involved, we further simplify the equations by considering

the thermodynamic limit. We take the number of atoms of spin  $\sigma$ ,  $N_\sigma$ , to infinity while keeping  $\bar{n}_\sigma$  constant. In this case, a useful approach is to use the factorized ansatz  $\rho = \bigotimes_l [\sum_m \rho_{m,l}(t) |m\rangle\langle m|]$ , where  $l$  labels the different sites. We further consider a translationally invariant system, and for this reason we will drop the  $l$  index in the following. The reduced single site density matrix  $\tilde{\rho} = \sum_m \tilde{\rho}_m(t) |m\rangle\langle m|$  has only one degree of freedom which we chose as the element  $\tilde{\rho}_{\uparrow\downarrow}(t)$ . The other elements follow from the knowledge of the filling and from the trace of  $\tilde{\rho}$  being unity. The elements of  $\tilde{\rho}$  are thus given by

$$\tilde{\rho}_0(t) = 1 - \bar{n}_\uparrow - \bar{n}_\downarrow + \tilde{\rho}_{\uparrow\downarrow}(t), \quad (72a)$$

$$\tilde{\rho}_\uparrow(t) = \bar{n}_\downarrow - \tilde{\rho}_{\uparrow\downarrow}(t), \quad (72b)$$

$$\tilde{\rho}_\downarrow(t) = \bar{n}_\uparrow - \tilde{\rho}_{\uparrow\downarrow}(t). \quad (72c)$$

Using Eq. (70), the time evolution of  $\tilde{\rho}_{\uparrow\downarrow}$  becomes

$$\begin{aligned} \frac{d\tilde{\rho}_{\uparrow\downarrow}}{dt} &= z \frac{d}{dt} (\tilde{\rho}_{\uparrow\downarrow}\tilde{\rho}_0 + \tilde{\rho}_{\uparrow\downarrow}\tilde{\rho}_\uparrow + \tilde{\rho}_{\uparrow\downarrow}\tilde{\rho}_\downarrow + \tilde{\rho}_{\uparrow\downarrow}\tilde{\rho}_{\uparrow\downarrow}) \\ &= -\left[ \frac{2J^2\gamma}{(\hbar\gamma)^2 + U^2} (2\tilde{\rho}_{\uparrow\downarrow}\tilde{\rho}_0 - \tilde{\rho}_\downarrow\tilde{\rho}_\uparrow - \tilde{\rho}_\uparrow\tilde{\rho}_\downarrow) \right. \\ &\quad \left. + \frac{2J^2}{\hbar\gamma^2} \left( \sum_{\sigma=\uparrow,\downarrow} \tilde{\rho}_{\uparrow\downarrow}\tilde{\rho}_\sigma - \tilde{\rho}_\sigma\tilde{\rho}_{\uparrow\downarrow} \right) \right] \\ &= -\frac{4zJ^2\gamma}{(\hbar\gamma)^2 + U^2} (\tilde{\rho}_{\uparrow\downarrow}\tilde{\rho}_0 - \tilde{\rho}_\downarrow\tilde{\rho}_\uparrow) \end{aligned} \quad (73)$$

where  $z$  is the lattice connectivity. Using Eqs. (72) we thus get

$$\frac{d\tilde{\rho}_{\uparrow\downarrow}(t)}{dt} = \gamma_{n,\text{ad}} (\bar{n}_\uparrow\bar{n}_\downarrow - \tilde{\rho}_{\uparrow\downarrow}(t)) \quad (74)$$

where  $\gamma_{n,\text{ad}} = \frac{8J^2\gamma}{\hbar^2\gamma^2 + U^2}$  for a one-dimensional lattice. It is worth noting the similarity between  $\gamma_{n,\text{ad}}$  and  $\lambda_{n,\text{Zeno}}$ . Eq. (74) is, as above expressed, consistent with the analytically derived steady state (Eqs. (7) through (10)), and is easily integrated to give

$$\tilde{\rho}_{\uparrow\downarrow}(t) = \bar{n}_\uparrow\bar{n}_\downarrow + (\tilde{\rho}_{\uparrow\downarrow}(0) - \bar{n}_\uparrow\bar{n}_\downarrow) e^{-\gamma_{n,\text{ad}}t}. \quad (75)$$

An exponential decay with a suppressed rate  $\gamma_{n,\text{ad}}$  is found which is in agreement with the two site result. As discussed for the two site case, the Zeno-effect induces a decreasing decay rate of  $J^2/(\hbar^2\gamma)$  for large bare coupling strength  $\gamma$ . Additionally, the interaction is found to slow down considerably the decay rate as  $\gamma J^2/U^2$  for large interaction strength. A similar dynamical effect had been observed in dissipative bosonic systems [11–15, 18].

We can further use the dynamics of the diagonal terms, to compute the coherence of the systems using Eq. (68). The time evolution of the coherence is given by

$$\begin{aligned} C(t) &= -\frac{8JU}{\hbar^2\gamma^2 + U^2} (\tilde{\rho}_{\uparrow\downarrow}\tilde{\rho}_0 - \tilde{\rho}_\downarrow\tilde{\rho}_\uparrow) \\ &= -\frac{8JU}{\hbar^2\gamma^2 + U^2} (\tilde{\rho}_{\uparrow\downarrow}(0) - \bar{n}_\uparrow\bar{n}_\downarrow) e^{-\gamma_{n,\text{ad}}t}, \end{aligned} \quad (76)$$

whereas the evolution equation for the fluctuations is given by

$$\begin{aligned} \kappa(t) &= (\tilde{\rho}_\downarrow(t) + \tilde{\rho}_\uparrow(t) + 4\tilde{\rho}_{\uparrow\downarrow}(t)) - (\tilde{n}_\uparrow + \tilde{n}_\downarrow)^2 \\ &= \{ \tilde{n}_\uparrow + \tilde{n}_\downarrow + 2 [\tilde{n}_\uparrow\tilde{n}_\downarrow + (\tilde{\rho}_{\uparrow\downarrow}(0) - \tilde{n}_\uparrow\tilde{n}_\downarrow)e^{-\gamma n_{\text{ad}}t}] \} \\ &\quad - (\tilde{n}_\uparrow + \tilde{n}_\downarrow)^2 \\ &= \kappa(\infty) + 2(\tilde{\rho}_{\uparrow\downarrow}(0) - \tilde{n}_\uparrow\tilde{n}_\downarrow)e^{-\gamma n_{\text{ad}}t} \end{aligned} \quad (77)$$

The presence of strong interaction can thus cause the dynamics to dramatically slow down as the characteristic exponent is inversely proportional to  $U^2$ .

## IV. DISSIPATIVE EVOLUTION

### A. Dissipative coupling to the local density

Dissipative coupling to the local density causes the fermionic system to heat up and to flow, at long times, towards the infinite temperature state, i.e. the totally mixed state proportional to unity in the Fock basis. Even though this final state is fairly simple, the evolution towards this state is very interesting and presents various features which depend on the interplay between the interaction, dissipation and hopping terms. We focus here on the evolution of the local kinetic energy as many of the interesting dynamical features are exemplified by this quantity. Within the slave-spin representation, at the mean-field level, the local kinetic energy is given by  $E_{\text{kin}}(t) = -J \sum_\sigma \langle c_{j,\sigma}^\dagger c_{j',\sigma} \rangle = -J_{\text{eff}} \sum_\sigma \langle S_\sigma^x(t) \rangle^2$ , where  $j$  and  $j'$  are neighboring sites. Whereas for the two fermions on two sites toy model, the kinetic energy is  $E_{\text{kin}}(t) = -2J \text{Re}[\rho_{13} + \rho_{23} - \rho_{14} - \rho_{24}]$  where the  $\rho_{ll'}$  are entries in the  $4 \times 4$  density matrix representing the system. For all situations considered here, we choose the initial state to be the ground state of the metallic phase, consequently  $E_{\text{kin}}(0) \neq 0$ . Such a phase exists in the range  $0 < U < 2J_{\text{eff}}$  when the  $d$ -dimensional fermionic system is represented within the mean-field slave-spin approach. In contrast, for the two fermions on two sites model, the kinetic energy is finite for all finite values of  $U/J$ .

When the evolution of the metallic state takes place in the absence of interaction, i.e. at  $U = 0$ , the kinetic energy decays exponentially as  $E_{\text{kin}}(t) = E_{\text{kin}}(0) e^{-\gamma t}$ . Within the slave-spin approach, using the Heisenberg picture for the master equation, this result is recovered and is illustrated in Fig. 2.

The presence of interaction alters this behavior. Typical evolutions of the kinetic energy for different interaction strengths, evaluated within the slave-spin approach, are illustrated in Fig. 2. As it can be seen on this figure, in addition to the exponential decay, the presence of interaction causes oscillations. For large interaction strengths,  $U \gg \hbar\gamma$ ,  $J_{\text{eff}}$ , the oscillation period is approximately inversely proportional to the interaction, i.e.  $T_p \approx \frac{4\pi\hbar}{U}$ . This finding is supported by an analysis of

the behavior of the eigenvalues extracted from the two-fermion, two-site system (see section III A 2). Whereas eigenvalues  $\lambda_{n,0}$ ,  $\lambda_{n,1}$ ,  $\lambda_{n,4}$  and  $\lambda_{n,\text{Zeno}}$  are purely real and therefore only cause an exponential decay, the imaginary parts of both  $\lambda_{n,2}$  and  $\lambda_{n,3}$  are proportional to  $\pm U/\hbar$  in the large  $U$  limit (see Fig. 4).

In the opposite limit, for small interaction strengths,  $U \ll \hbar\gamma$ ,  $J$ , the imaginary parts of  $\lambda_{n,2}$  and  $\lambda_{n,3}$  exhibit a different behavior. To linear order in  $U$ , we find that the imaginary parts go as  $\sim \mp 4J/\hbar$  for  $4J \gg \hbar\gamma$ ,  $U$  while  $\sim \mp U/\hbar$  for  $\hbar\gamma \gg 4J$ ,  $U$ . The behavior of both  $\lambda_{n,2}$  and  $\lambda_{n,3}$  is illustrated in Fig. 5: for  $U = 0.1J$  and  $\hbar\gamma \gg 4J$  the imaginary parts of these eigenvalues are approximately equal to  $\pm U/\hbar$ , whereas for  $\hbar\gamma < 4J$  their imaginary parts grow rapidly to  $\pm 4J/\hbar$ . For a system made of many sites, the dependence of the oscillation frequency of the kinetic energy with increasing  $\gamma$  is seen in Fig. 3 (result obtained using the slave-spin approach). At low  $\gamma = 0.01\hbar/J_{\text{eff}}$ , fast oscillations (with a weak amplitude) can be seen in Fig. 3 (a) compared to slower oscillations evident in the logarithmic scale in Fig. 3 (b) for  $\gamma = 0.1\hbar/J$ . This figure also shows that in an extended systems, at low interaction strength, the exponential decay of the kinetic energy,  $E_{\text{kin}}(t) \propto e^{-\gamma t}$ , exact for  $U = 0$ , still holds for the oscillation envelope.

However, in Fig. 3, an initial decay rate slightly larger than  $\gamma$  can be seen. To understand this deviation, we analyze the structure of the real parts of the eigenvalues for the system of two fermions on two sites. We find that the real parts of eigenvalues  $\lambda_{n,2}$  and  $\lambda_{n,3}$  are approximately  $-\gamma$ . However, the real part of  $\lambda_{n,1}$  and, for large  $\gamma$ , the real part of  $\lambda_{n,4}$  both take value close to  $-2\gamma$ . This is clearly depicted in Fig. 5.

The behavior of the real part of  $\lambda_{n,\text{Zeno}}$  is even more fascinating: for  $\hbar\gamma$ ,  $U \gg J$ , this eigenvalue approaches zero as  $\lambda_{n,\text{Zeno}} = -\frac{8\gamma J^2}{(\hbar\gamma)^2 + U^2}$  (see Figs. 4 and 5). This result implies that the components of the density matrix which overlap with the corresponding eigenvector become very stable and the system evolves very slowly. Therefore, the system dynamics exhibits two regimes: a short time exponential decay with a rate proportional to  $\gamma$  and a long time decay dominated by the rate  $\lambda_{n,\text{Zeno}}$ . In Fig. 6, the presence of these two regimes can be seen in the time-evolution of the kinetic energy for the two-site system.

The long time exponential decay of the kinetic energy with rate  $\lambda_{n,\text{Zeno}}$  is also recovered in the extended system when its evolution is analyzed using the adiabatic elimination technique (see section III C). Within this approach, a simple picture for the origin of this effect is gained by interpreting the dissipative coupling as a measurement process. A large dissipative coupling acts as a projection onto the dissipation free subspace where no evolution occurs. Therefore, at long times, the state evolution is slowed down by the dissipative measurement as it is inevitably close to the dissipation free subspace. In contrast to the usual Zeno picture which also occurs in absence of interaction, in the fermionic systems under

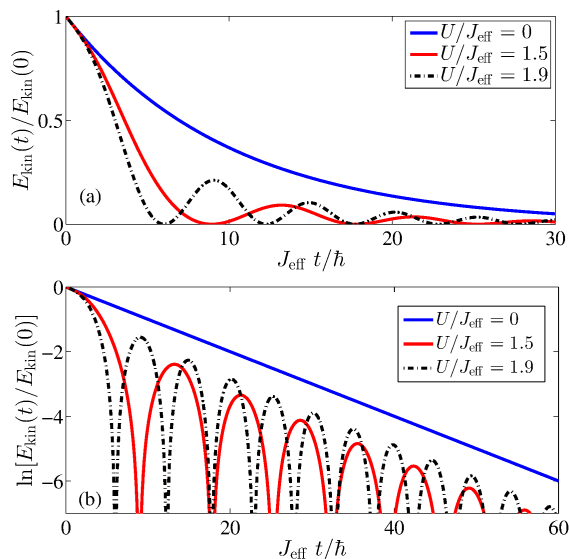


FIG. 2: (Color online): Time-evolution of the normalized kinetic energy for a dissipative coupling  $\hbar\gamma = 0.1J_{\text{eff}}$  to the local density and for various interaction strengths in (a) linear scale and (b) log scale. These results are obtained within the slave-spin approach solving Eqs. (46) to (49). The evolution begins from the metallic ground state of the mean-field Hamiltonian describing the charge sector (Eq. (43)) with  $Z(t=0) = 1, 0.44, 0.098$  for  $U/J_{\text{eff}} = 0, 1.5, 1.9$  respectively.

study an additional process occurs due to the presence of strong interactions. For large interaction strengths, the decay rate is suppressed as  $\gamma J^2/U^2$ . This strong suppression of the decay rate can be understood by considering the balance of energy. Decoherence is caused by the proliferation of excitations, a process requiring a large amount of (interaction) energy. As this energy can only be injected into the system by the dissipative process itself, very few excitations are generated.

Within the slave-spin approach, only a weak dependence of the decay rate on the interaction strength is observed (Fig. 2) and the Zeno effect is not visible. We attribute this situation to the single-site mean-field decoupling used to study the system evolution within the slave-spin approach. Due to this mean-field decoupling,  $\langle S_i^x \rangle$  decays rapidly for large dissipative couplings to the local density: the connection to the bath of sites is therefore suppressed and the system freezes artificially. The use of such mean-field approximations can thus result in the appearance of artificial steady states that are not the true long time limits, consequently these approximations must be used with great care. However, the absence of the Zeno effect in this particular case is not a fundamental flaw of the slave-spin approach as it is due to our drastic mean-field decoupling. In fact, we will see in the next section that, for a dissipative coupling to the double occupation, the Zeno effect is recovered within the slave-spin approach even at the level of the single-site

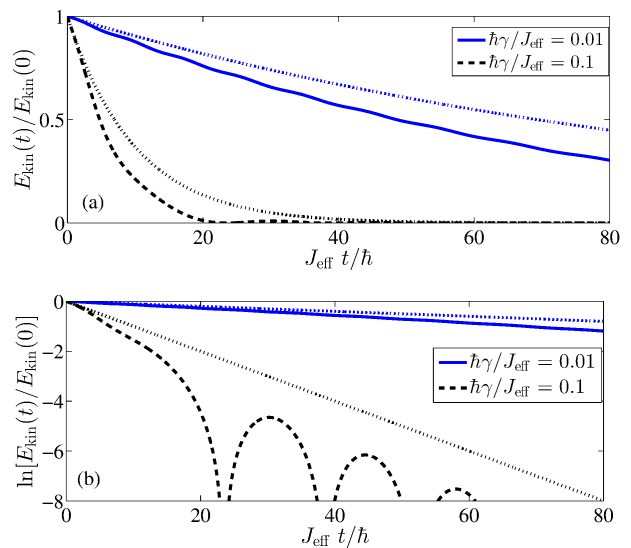


FIG. 3: (Color online): Time-evolution of the normalized kinetic energy for different dissipative couplings to the local density for an interaction strength  $U = J_{\text{eff}}$  in (a) linear scale and (b) log scale. The results are obtained within the slave-spin approach solving Eqs. (46) to (49). Here again the evolution begins from the metallic ground state of the mean-field Hamiltonian describing the charge sector (Eq. (43)) with  $Z(t=0) = 0.75$  for  $U = J_{\text{eff}}$ . The two dotted lines denote pure exponential decay  $\propto e^{-\gamma t}$  for  $\hbar\gamma/J_{\text{eff}} = 0.01$  and  $0.1$ .

mean-field decoupling.

## B. Dissipative coupling to the local double occupancy

Similarly to the coupling to the local density, a dissipative coupling to the local double occupancy also causes the fermionic system to heat up. However, in the latter case, the steady state occurring in the long time limit depends crucially on the initial state. In particular, we find that the single particle coherence can survive even under the presence of dissipation, and that the final state is a combination of the infinite temperature state and of eigenstates of the kinetic part of the Hamiltonian. This eigenstate possesses this special feature that it is only made of singly occupied sites.

One of the remarkable features of this dynamics, clearly noticeable in Fig. 7, is the long-time slowing down of the decay rate with increasing dissipative coupling strength. Within the two-fermion on two-site model, this slowing down corresponds to the occurrence of an eigenvalue,  $\lambda_{d,\text{Zeno}}$ , having a real part proportional to  $-\frac{24\gamma J^2}{(\hbar\gamma)^2 + 4U^2}$  (up to second order in  $J$ ). For the case of large dissipative coupling, when  $\hbar\gamma \gg U$ , the real part of this eigenvalue becomes proportional to  $-\frac{J^2}{\hbar^2\gamma}$  and corresponds to the previously discussed Zeno effect (see

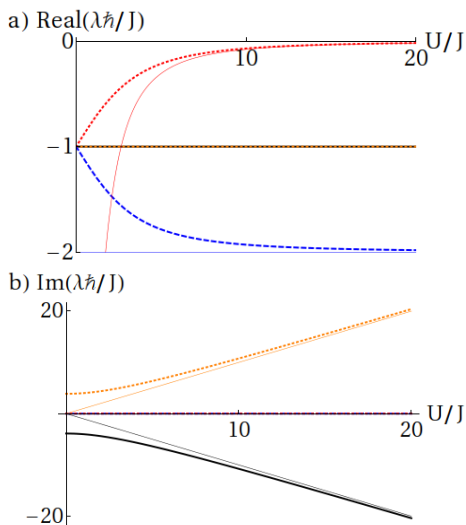


FIG. 4: (Color online) Real (a) and imaginary (b) parts for  $\lambda_{n,2}$  (solid black),  $\lambda_{n,3}$  (dotted orange),  $\lambda_{n,4}$  (dashed blue) and  $\lambda_{n,\text{Zeno}}$  (dotted red) versus  $U/J$  for a system of two fermions (one spin up and one spin down) on two sites with dissipative coupling  $\hbar\gamma/J = 1$  to the local density. The solid thin lines correspond to analytical predictions for the real parts  $-8\gamma J^2/[(\hbar\gamma)^2 + U^2]$  (red) and  $-2\gamma$  (blue), and for the imaginary parts  $U/\hbar$  (orange) and  $-U/\hbar$  (black). The real parts of  $\lambda_{n,2}$  and  $\lambda_{n,3}$  are both equal to  $-J/\hbar$  whereas the imaginary parts of both  $\lambda_{n,4}$  and  $\lambda_{n,\text{Zeno}}$  are null.

Fig. 8).

Surprisingly, within the slave-spin approach, the decay rate is found to adopt an algebraic form for  $U = 0$ . For the case of an instantaneous quench to the non-interacting limit, the slave-spin differential equation can be solved analytically, and we find the kinetic energy to decay as  $\frac{1}{\gamma t}$ . The numerical simulations at small  $\gamma$  provide support for the presence of similar algebraic decays even for slightly larger interaction strengths. However, for these cases the identification of the exact mathematical form is a much more difficult task. Nevertheless, we can clearly see in Fig. 9 that the asymptotic long-time state at large dissipative couplings or large interaction strengths still possesses a large amount of kinetic energy, an observation that is in agreement with our predictions obtained in the analytically solvable limits. An investigation using the adiabatic elimination method could clarify the exact form of the decay and the properties of this new steady state; however, due to the high dimensional decoherence free subspace, which complicates the situation considerably, such a study is beyond the scope of the current work.

Finally, the evolution of the kinetic energy within the slave-spin approach is characterized by the presence of oscillations at finite interaction strengths. The frequency of these oscillations is approximately proportional to  $U/\hbar$  for very large interaction values as can be seen in Fig. 9. However, for small values of  $U$ , the oscillation frequency decreases with increasing values of the dissipative cou-

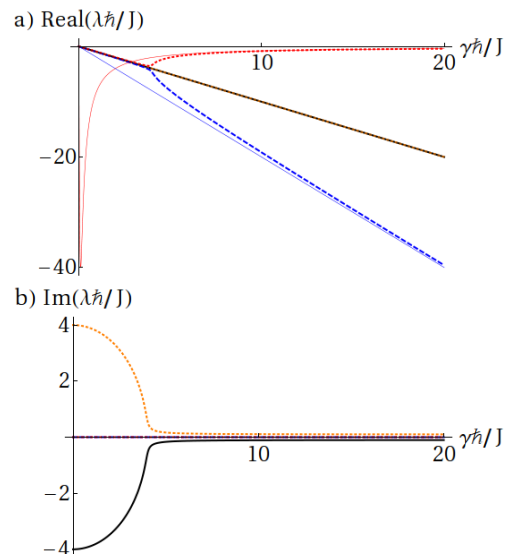


FIG. 5: (Color online): Real (a) and imaginary (b) parts for  $\lambda_{n,2}$  (solid black),  $\lambda_{n,3}$  (dotted orange),  $\lambda_{n,4}$  (dashed blue) and  $\lambda_{n,\text{Zeno}}$  (dotted red) versus  $\hbar\gamma/J$  for a system of two fermions (one spin up and one spin down) on two sites with interaction strength  $U/J = 0.1$  and dissipative coupling to the local density. The solid thin lines correspond to analytical predictions for the real parts  $-8\gamma J^2/[(\hbar\gamma)^2 + U^2]$  (red) and  $-2\gamma$  (blue). The imaginary parts of both  $\lambda_{n,4}$  and  $\lambda_{n,\text{Zeno}}$  are null.

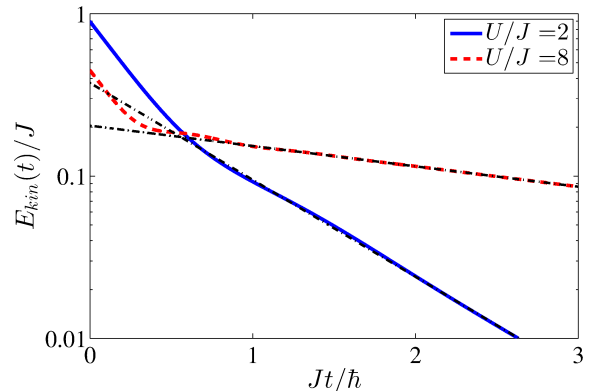


FIG. 6: (Color online): Time-evolution of the kinetic energy for a two-site two-fermion system with a dissipative coupling  $\hbar\gamma/J = 3$  to the local density. This figure highlights the presence of two regimes: a short time exponential decay with a rate proportional to  $\gamma$  and a long time decay dominated by the rate  $\lambda_{n,\text{Zeno}}$ . The black dash-dotted lines are the corresponding Zeno predictions.

pling,  $\gamma$  (see Fig. 7). For the two-fermion on two-site system, this result corresponds to the saturation, at small  $U$ , of the imaginary parts of eigenvalues  $\lambda_{d,4}$  and  $\lambda_{d,\text{Zeno}}$  as shown in Fig. 10.

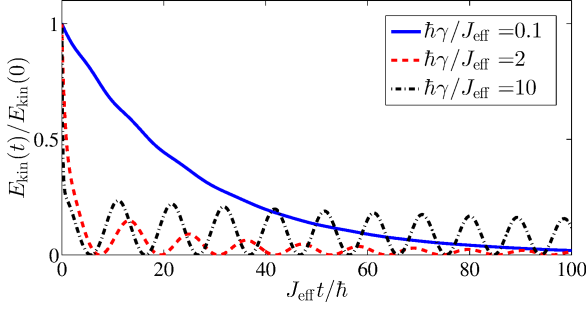


FIG. 7: (Color online): Time-evolution of the normalized kinetic energy for an interaction strength  $U = J_{\text{eff}}$  and different dissipative couplings to the local double occupancy. The results are obtained within the slave-spin approach solving Eqs. (54) to (60). The evolution begins from the metallic ground state of the mean-field Hamiltonian describing the charge sector (Eq. (43)) with  $Z(t=0) = 0.75$  for  $U = J_{\text{eff}}$ .

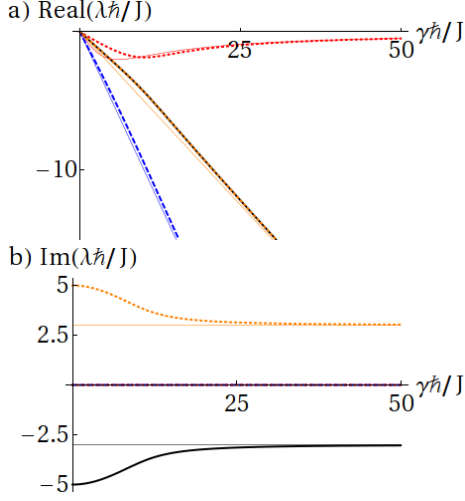


FIG. 8: (Color online): Real (a) and imaginary (b) parts for  $\lambda_{d,1}$  (dashed blue),  $\lambda_{d,2}$  (black),  $\lambda_{d,3}$  (dotted orange) and  $\lambda_{n,\text{Zeno}}$  (dotted red) versus  $\hbar\gamma/J$  for two fermions (one spin up and one spin down) on two sites with  $U/J = 3$  and dissipative coupling to the local double occupancy. The solid thin lines correspond to analytical predictions for the real parts  $-24\gamma J^2/[(\hbar\gamma)^2 + U^2]$  (red),  $-\gamma/2$  (orange),  $-\gamma$  (blue), and for the imaginary parts  $-U/\hbar$  (black) and  $U/\hbar$  (orange). The imaginary parts of both  $\lambda_{d,1}$  and  $\lambda_{d,\text{Zeno}}$  are null.

## V. CONCLUSION

We investigated the dynamics of strongly interacting fermions in a lattice and submitted to dissipative effects. We studied in detail two kinds of dissipative processes: in the first situation, the environment is effectively coupled to the local fermionic density whereas, in the second case, the dissipative coupling is to the local double occupancy. As a preamble, we analyzed a system of two atoms (one for each spin) on two sites in order to obtain initial insights into the dynamics of these open sys-

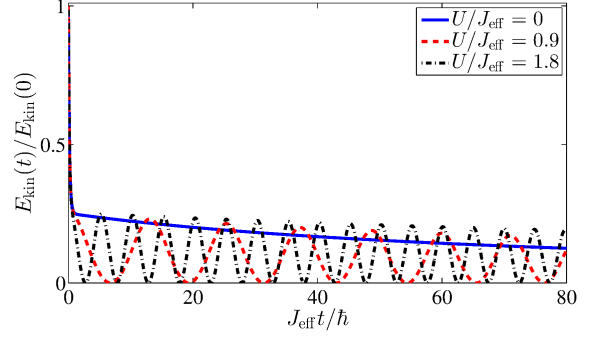


FIG. 9: (Color online): Time-evolution of the normalized kinetic energy for a dissipative coupling  $\hbar\gamma/J_{\text{eff}} = 10$  to the local double occupancy and different interaction strengths. The results are obtained within the slave-spin approach solving Eqs. (54) to (60). Here again the evolution begins from the metallic ground state of the mean-field Hamiltonian describing the charge sector (Eq. (43)) with  $Z(t=0) = 0, 0.8, 0.998$  for  $U/J_{\text{eff}} = 0, 0.8, 1.9$  respectively.

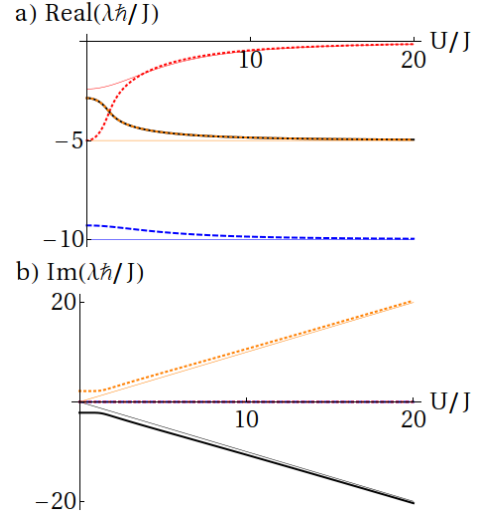


FIG. 10: (Color online): Real (a) and imaginary (b) parts for  $\lambda_{d,1}$  (dashed blue),  $\lambda_{d,2}$  (black),  $\lambda_{d,3}$  (dotted orange) and  $\lambda_{n,\text{Zeno}}$  (dotted red) versus  $U/J$  for two fermions (one spin up and one spin down) on two sites with dissipative coupling  $\hbar\gamma/J = 10$  to the local double occupancy. The solid thin lines correspond to analytical predictions for the real parts  $-24\gamma J^2/[(\hbar\gamma)^2 + U^2]$  (red),  $-\gamma/2$  (orange),  $\gamma$  (blue), and for the imaginary parts  $-U/\hbar$  (black) and  $U/\hbar$  (orange). The imaginary parts of both  $\lambda_{d,1}$  and  $\lambda_{d,\text{Zeno}}$  are null.

tems. We then developed a novel method to study the short-time dynamics of fermionic many-body open systems based on a slave-spin representation of the interacting fermions. In parallel, for the case of fermions with a dissipative coupling to the local density, we pursued a radically different approach and explored their dynamics using adiabatic elimination. This method is designed to work well at long times and complements well the mean-

field slave-spin approach. We applied these techniques to the two types of dissipative processes, and found that in both cases it is possible to highlight the presence of slow decaying states occurring due to the Zeno-effect or to “interaction impeding” (also referred to as “interaction Zeno-effect”). We were also able to identify important properties of the steady states. In particular, for the coupling to the local density, we found that the steady state is unique and is the infinite temperature state. We also predicted that, for dissipation coupled to the density, the short time dynamics (from the ground state of the fermionic Hamiltonian) is characterized by an exponential decay with oscillations whose period dependent on the interaction strength  $U$ . For the local coupling to the double occupancy, we found that, unlike in the previous case, the steady state is not unique and depends on the initial condition. The presence of coherence at long times also allows for a more reliable use of the slave-spin method while it greatly complicates the use of the adiabatic elimination approach. For this last coupling, we observed an exponentially decaying behavior which depends on  $U$ . The mean-field slave-spin approach also predicts the presence of a power law decay when the dissipative system is quenched to the non-interacting limit.

However, this interesting result remains to be confirmed using a complementary approach, which is left to future work. To conclude, we believe that the slave-spin method developed here, and benchmarked against other reliable approaches, provides a new and exciting framework to study notoriously complex systems: interacting lattice fermions coupled to a dissipative environment.

*Note:* During the final stage of this work, a complementary article (Ref. 36) appeared online. The authors of this article derived the Master equation for the fermionic atoms with a coupling to the local density. Additionally, an analysis of the two-site and one-dimensional fermionic systems was performed using a combination of the stochastic wave function method and of the density-matrix renormalization group.

### Acknowledgments

We thank A. Georges for his contributions to the early stage of this work. We acknowledge BCGS, DFG, CIFAR (Canada), MOE Singapore start-up grant and NSERC of Canada for their financial support.

- 
- [1] Fluorescence scattering is the absorption of a (lattice) photon by an atom which is then followed by a spontaneous emission.
  - [2] D. Fausti, R. I. Tobey, N. Dean, S. Kaiser, A. Dienst, M. C. Hoffmann, S. Pyon, T. Takayama, H. Takagi, and A. Cavalleri, *Science* **331**, 189 (2011).
  - [3] E. W. Streed, J. Mun, M. Boyd, G. K. Campbell, P. Medley, W. Ketterle, and D. E. Pritchard, *Phys. Rev. Lett.* **97**, 260402 (2006).
  - [4] N. Syassen, D. M. Bauer, M. Lettner, T. Volz, D. Dietze, J. J. Garcia-Ripoll, J. I. Cirac, G. Rempe, and S. Dürr, *Science* **320**, 1329 (2008).
  - [5] J. T. Barreiro, M. Miller, P. Schindler, D. Nigg, T. Monz, M. Chwalla, M. Hennrich, C. F. Roos, P. Zoller, and R. Blatt, *Nature* **470**, 486 (2010).
  - [6] M. Müller, S. Diehl, G. Pupillo, and P. Zoller, *Advances in Atomic, Molecular, and Optical Physics* **61**, 1 (2012).
  - [7] R. C. F. Caballar, S. Diehl, H. Mäkelä, M. Oberthaler, and G. Watanabe, *Phys. Rev. A* **89**, 013620 (2014).
  - [8] J.-S. Bernier, P. Barmettler, D. Poletti, and C. Kollath, *Phys. Rev. A* **87**, 063608 (2013).
  - [9] A. Daley, arXiv:1405.6694 (2014).
  - [10] G. K. Brennen, G. Pupillo, A. M. Rey, C. W. Clark, and C. J. Williams, *Journal of Physics B: Atomic, Molecular and Optical Physics* **38**, 1687 (2005).
  - [11] H. Pichler, A. J. Daley, and P. Zoller, *Phys. Rev. A* **82**, 063605 (2010).
  - [12] D. Poletti, J.-S. Bernier, A. Georges, and C. Kollath, *Phys. Rev. Lett.* **109**, 045302 (2012).
  - [13] V. S. Shchesnovich and V. V. Konotop, *Phys. Rev. A* **81**, 053611 (2010).
  - [14] V. A. Brazhnyi, V. V. Konotop, V. M. Pérez-García, and H. Ott, *Phys. Rev. Lett.* **102**, 144101 (2009).
  - [15] D. Witthaut, F. Trimborn, H. Hennig, G. Kordas, T. Geisel, and S. Wimberger, *Phys. Rev. A* **83**, 063608 (2011).
  - [16] J. J. Mendoza-Arenas, T. Grujic, D. Jaksch, and S. R. Clark, *Phys. Rev. B* **87**, 235130 (2013).
  - [17] S. Kessler, A. Holzner, I. P. McCulloch, J. von Delft, and F. Marquardt, *Phys. Rev. A* **85**, 011605 (2012).
  - [18] D. Poletti, P. Barmettler, A. Georges, and C. Kollath, *Phys. Rev. Lett.* **111**, 195301 (2013).
  - [19] Z. Cai and T. Barthel, *Phys. Rev. Lett.* **111**, 150403 (2013).
  - [20] A. Tomadin, S. Diehl, and P. Zoller, *Phys. Rev. A* **83**, 013611 (2011).
  - [21] B. Olmos, I. Lesanovsky, and J. Garrahan, *Phys. Rev. Lett.* **109**, 020403 (2012).
  - [22] I. Lesanovsky and J. P. Garrahan, *Phys. Rev. Lett.* **111**, 215305 (2013).
  - [23] L. de’Medici, A. Georges, and S. Biermann, *Phys. Rev. B* **72**, 205124 (2005).
  - [24] F. Gerbier and I. Castin, *Phys. Rev. A* **82**, 013615 (2010).
  - [25] C. Gardiner and P. Zoller, *Quantum Noise* (Springer-Verlag, 2000).
  - [26] H. Carmichael, *An open systems approach to quantum optics* (Springer Verlag, 1991).
  - [27] H. P. Breuer and F. Petruccione, *The theory of open quantum systems* (Oxford University Press, Oxford, 2002).
  - [28] M. Köhl, H. Moritz, T. Stöferle, K. Günter, and T. Esslinger, *Phys. Rev. Lett.* **94**, 080403 (2005).
  - [29] I. Bloch, J. Dalibard, and W. Zwerger, *Rev. Mod. Phys.* **80**, 885 (2008).
  - [30] N. W. Ashcroft and N. D. Mermin, *Solid State Physics* (Saunders College Publishing, 1976).

- [31] S. Florens and A. Georges, Phys. Rev. B **66**, 165111 (2002).
- [32] S. R. Hassan and L. de' Medici, Phys. Rev. B **81**, 035106 (2010).
- [33] T. Barthel, New Journal of Physics **15**, 073010 (2013).
- [34] J. J. Garcia-Ripoll, S. Drr, N. Syassen, D. M. Bauer, M. Lettner, G. Rempe, and J. I. Cirac, New Journal of Physics **11**, 013053 (2009).
- [35] K. Saito and Y. Kayanuma, Phys. Rev. A **65**, 033407 (2002).
- [36] S. Sarkar, S. Langer, J. Schachenmayer, and A. J. Daley, arXiv:1405.7336 (2014).